

# PERFORMANCE EVALUATION OF ANN-BASED AND CONVENTIONAL PI-CONTROLLED SHUNT ACTIVE POWER FILTERS FOR POWER QUALITY IMPROVEMENT USING P-Q THEORY

Gaurav Ved, Kapil Parikh

E-Mail Id: vedgaurav331@gmail.com

Department of Electrical Engineering, SITE Nathdwara, Rajasthan, India

**Abstract-** This paper presents a basic Artificial Neural Network (ANN)-based control approach for shunt active power filters (SAPFs) to mitigate harmonic currents and improve power factor. Power quality (PQ) issues, such as harmonic distortion, have become a major challenge due to the increasing prevalence of nonlinear loads and electronic devices, affecting the efficiency, performance, and lifespan of electrical equipment. To address this, a MATLAB/Simulink-based dynamic model of an ANN-controlled SAPF has been developed. The study focuses on enhancing PQ by reducing harmonic disturbances under unbalanced load conditions. Through detailed simulations, the proposed ANN-controlled SAPF is evaluated under various scenarios, including linear and nonlinear loads, and compared with a conventional Proportional-Integral (PI) controller. Performance metrics such as harmonic distortion reduction, response time, system stability, and adaptability are analyzed. The study also examines hysteresis and PI controllers while comparing three-phase ANN-controlled SAPFs. Results demonstrate the superior performance of ANN-controlled SAPFs in improving PQ and reducing harmonic distortion, offering valuable insights for industrial applications.

**Keywords:** ANN, SAPF, PI, THD, FFT, PQ.

## 1. INTRODUCTION

An electrical load at the consumer end should consistently receive continuous power of high quality under normal operating conditions. Any disturbance in system voltage or frequency directly affects consumer loads, making it crucial to maintain these parameters at their scheduled values. This study provides a comprehensive evaluation of active filters, including control strategies, configurations, component selection, economic and technical considerations, and their suitability for specialized applications.

The simulation of a Shunt Active Power Filter (SAPF) is performed using an indirect current control technique, applicable under both balanced and unbalanced three-phase voltage source conditions with a variable speed drive. A comparative analysis of various hybrid active filters is conducted, focusing on their technologies, control algorithms, and ratings. A customized "p-q" theory is proposed for harmonic extraction under distorted voltage conditions, enhancing practical application.

An ideal Phase-Locked Loop (PLL) circuit integrated with PI, PID, or Fuzzy Logic Controller (FLC)-based shunt Active Power Line Conditioner (APLC) is presented to improve power quality by mitigating current harmonics and compensating for reactive power under unbalanced variable loads. The shunt APLC system, implemented with a three-phase current-controlled Voltage Source Inverter (VSI), is connected at the point of common coupling to inject equal but opposite filter currents, thereby compensating current harmonics. Hysteresis Current Control (HCC) generates switching pulses for the VSI. A detailed comparative assessment of the three control techniques—PI, PID, and FLC—is provided, highlighting their performance in improving power quality.

Several innovative Hybrid Active Power Filter (H-APF) approaches have been proposed to improve power quality by utilizing various control strategies and compensation techniques for different load types. Belaidi et al. introduced a three-phase shunt-APF with fuzzy logic control (FLC) to compensate for imbalanced source voltages, using a phase-locked loop (PLL) for voltage regulation and hysteresis current control (HCC) for gate pulse generation. Thuyen employed the social spider algorithm (SSA) for inverter current measurement, along with PQ-theory and PWM to compute reference current. Behera et al. developed a fuzzy-based PI controller in a three-phase hybrid filter for harmonic mitigation, improving transient performance with vector-based PI controllers. Chau et al. proposed an H-APF with an adaptive current controller for better harmonic cancellation and dynamic response, while Kumar and Bhat's hybrid filter with FLC improved DC voltage settling time. Research on artificial neural network (ANN)-based methods for large-scale power systems is limited. Choudhary et al. introduced a single-phase S-APF using an ANN-based strategy, outperforming predictive controllers in THD reduction. Shahalami and Hosseini designed an ANN controller for H-APF to minimize processing time, and Pedepkeni et al. compared neural fuzzy control with traditional PI controllers for THD improvement. Sahu and Mahapatra developed a Virtex-5 FPGA-based DSTATCOM for reactive power compensation and harmonic mitigation. Hardware solutions like these offer potential improvements in power

DOI Number: <https://doi.org/10.30780/IJTRS.V10.I01.001>

pg. 1

[www.ijtrs.com](http://www.ijtrs.com), [www.ijtrs.org](http://www.ijtrs.org)

Paper Id: IJTRS-V10-I01-001

Volume X Issue I, January 2025

@2017, IJTRS All Right Reserved

quality, addressing current software-based limitations.

This paper presents a comprehensive dynamic model developed in MATLAB/Simulink to simulate the operation of an Artificial Neural Network (ANN)-controlled shunt active power filter (SAPF). The primary goal of the model is to enhance power quality in electrical systems by mitigating harmonic disturbances, especially under unbalanced load conditions. Through detailed simulations, the performance of the ANN-based control algorithm is evaluated across various operating scenarios, including linear and nonlinear load conditions. A comparative analysis is also conducted to emphasize the benefits of the ANN-controlled SAPF compared to a conventional Proportional-Integral (PI) controller. This study provides an in-depth examination of key parameters such as harmonic distortion reduction, response time, system stability, and adaptability to varying load conditions. The findings demonstrate the superior effectiveness of the ANN-controlled filter in improving power quality, offering significant insights for the optimization of modern power systems.

## 2. PROBLEM STATEMENT

A power system is a vast and complex network, often faced with various challenges that disrupt its smooth operation. One critical issue is harmonic distortion, primarily caused by nonlinear loads. Harmonics distort the sinusoidal waveforms of voltage and current, leading to significant disruptions in system parameters. Harmonics are broadly categorized into voltage and current harmonics in industrial systems. Current harmonics, for example, can overload the neutral conductor, typically by a factor of three, due to unbalanced currents that are not 120 degrees out of phase. This imbalance often results in the overloading of connected transformers, inducing eddy currents in the primary winding and increasing total transformer losses at full load, as these losses are proportional to line current. Additionally, in transformers with delta windings, third-order harmonics circulate within the winding, compounding existing losses. Ground faults caused by harmonics can also trip circuit breakers, further complicating system stability. Voltage harmonics, on the other hand, arise from interference due to current harmonics, leading to voltage drops across the source impedance. These distorted voltage waveforms impact all connected loads, forcing them to generate additional harmonic currents. The resulting eddy current losses in transformers escalate further, amplifying energy losses and operational inefficiencies. High noise levels from harmonic-generating equipment exacerbate these issues, creating significant challenges for system reliability and performance.

## 3. HARMONIC DISTORTION

- Harmonic distortion consists of higher frequency components that are integral multiples of the fundamental frequency of the signal.
- These harmonics are considered unwanted disturbances in the primary periodic waveform of the signal.
- The harmonic components mimic the waveform of the fundamental signal; if the fundamental is sinusoidal, the harmonics are also sinusoidal.
- Total Harmonic Distortion (THD) is a measure of the extent of harmonic distortion present in the system.

$$\text{THD} = \frac{\sqrt{(I_2^2 + I_3^2 + I_4^2 + \dots)}}{I_1} \times 100\%$$

$$= \frac{\sqrt{\sum_{h=2}^{\infty} I_h^2}}{I_1} \times 100\%$$

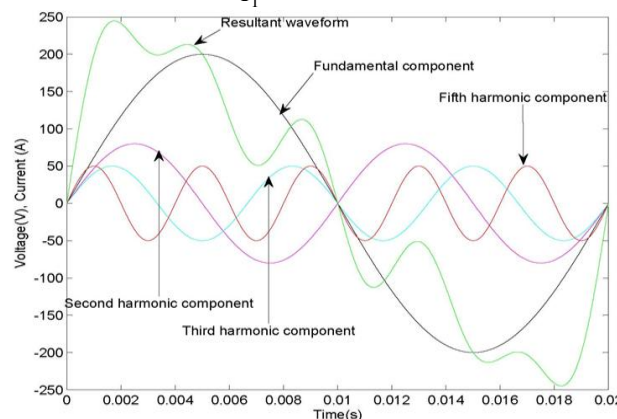


**Fig. 3.1 Components of Harmonics Present in Power System**

Active Filters (AF) are increasingly integrated into power networks to address harmonic issues. Over the past decades, advancements in technology and improvements in power electronics have driven a focus on delivering high-quality, reliable power for consumers and industries. However, devices such as computers, printers, photocopiers, CFLs, and

other commercial equipment, commonly referred to as variable loads, generate significant harmonic distortion. These variable loads create harmonics by drawing current in short pulses rather than in a smooth sinusoidal manner. Harmonics in non-linear loads contribute to elevated operating temperatures and insulation failure in generating equipment and transformers, leading to damage and potential blackouts over large areas. To address these challenges, Active Filters offer an effective solution for mitigating harmonics in non-linear loads, though their installation can be cost-prohibitive due to complexities in the distribution network.

In this work, a Shunt Active Power Filter (SAPF) is examined and modeled to accurately compensate for current harmonics. The PQ theory is employed, providing effective control and ensuring improved performance in the power system. The model is developed for a two-bus system with variable loads. Simulations are performed to verify the SAPF's performance under varying harmonic disturbances, with results validated using multiple waveforms and output analyses.

#### 4. SIMULATION AND RESULT ANALYSIS

The simulation results emphasize the effectiveness of the ANN-controlled shunt active power filter (SAPF) in improving power quality and reducing harmonics under diverse load conditions. The proposed ANN-based algorithm achieves lower Total Harmonic Distortion (THD) compared to the conventional PI controller, ensuring superior harmonic mitigation. Case studies demonstrate the ANN-controlled filter's ability to adapt rapidly and effectively to dynamic load variations, maintaining system stability and consistent performance. In contrast, the PI controller exhibits slower response times and diminished accuracy in complex scenarios. The ANN-based SAPF's robustness and adaptability make it a more efficient solution for addressing power quality challenges in modern grids.

Fig. 4.1 illustrates the Simulink model of the ANN-controlled SAPF, featuring a three-phase grid, linear and nonlinear load blocks, and additional dynamic loads. At the point of common coupling (PCC), the SAPF compensates for current distortions, enhancing system stability and mitigating harmonics effectively.

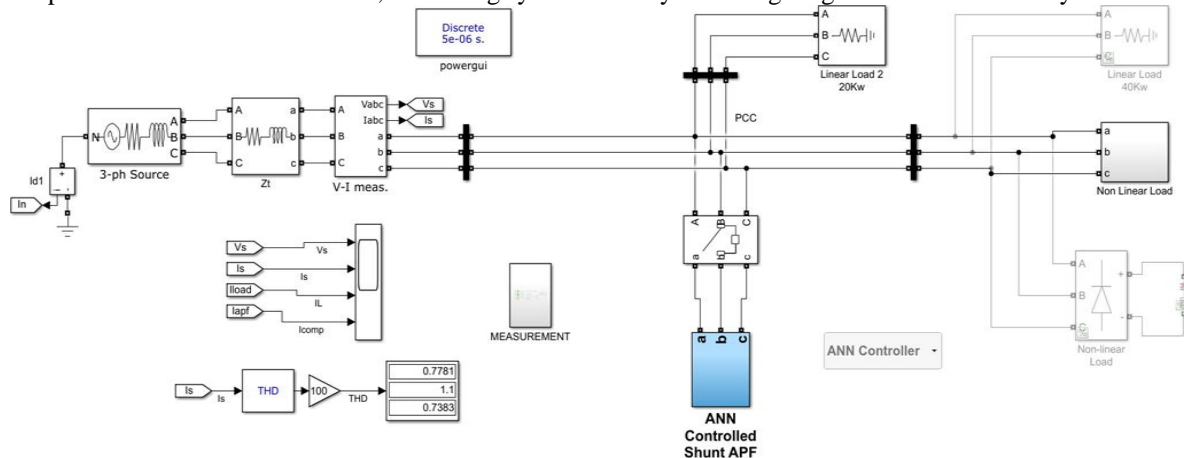


Fig. 4.1 Simulink model of the proposed ANN-controlled SAPF

#### Case-1: Simulation response of 3- $\Phi$ ANN-Controlled SAPF at Linear Load Condition

The simulation results for the proposed control algorithm are obtained under balanced linear load conditions. The system consists of two parallel-connected loads, rated at 40 kW and 20 kW, respectively. This configuration evaluates the algorithm's ability to manage power quality and ensure efficient load sharing. The results, presented in the following figures, highlight the algorithm's effectiveness in maintaining system stability and delivering high-quality power to the loads, demonstrating its suitability for balanced linear load scenarios.

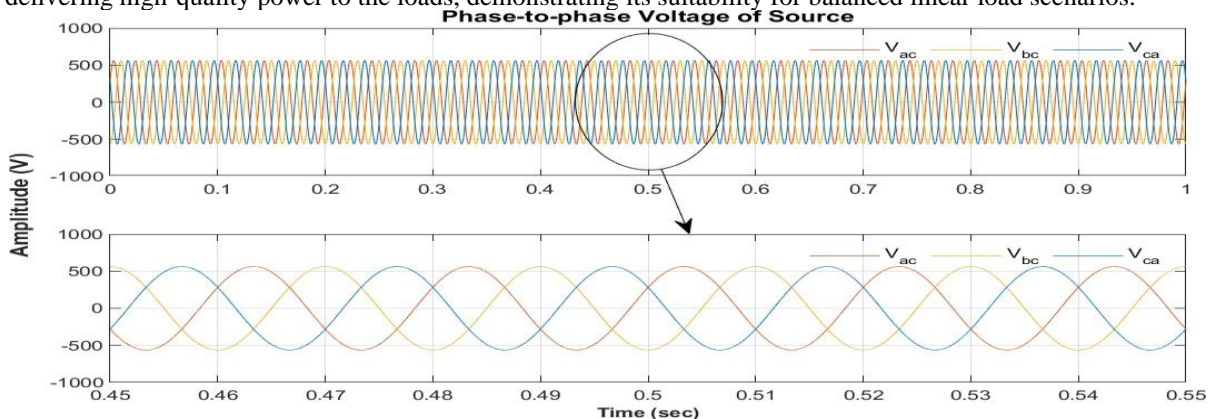


Fig. 4.2 Simulation result of phase-phase voltage of the source



Figures 4.2 and 4.3 show the phase-to-phase voltage and line current of the source under linear load conditions, with zoomed-in views highlighting the quality of the signals. The results indicate that both the source voltage and current maintain pure sinusoidal waveforms throughout the simulation. The voltage remains around 565 V, and the current is approximately 120 A. The zoomed-in sections, from  $t = 0.45$  sec to  $t = 0.55$  sec, emphasize the waveform purity, confirming the control algorithm's ability to maintain system stability and efficiency.

Figures 5 and 6 display the phase-to-phase voltage and line current of the load, respectively. Throughout the simulation, the voltage remains around 565 V, while the current is approximately 80 A.

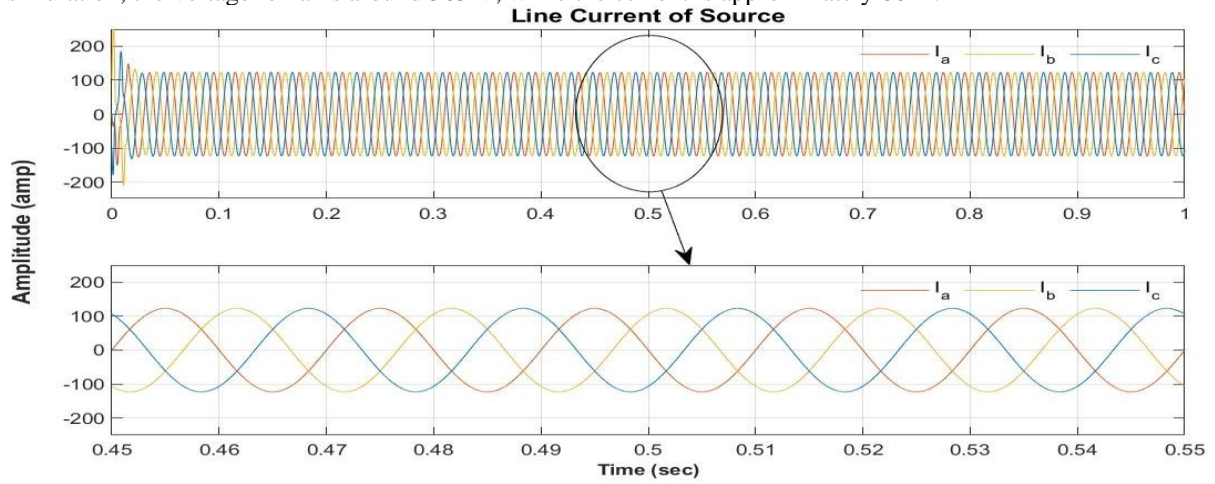


Fig. 4.3 Simulation result of line current of the source

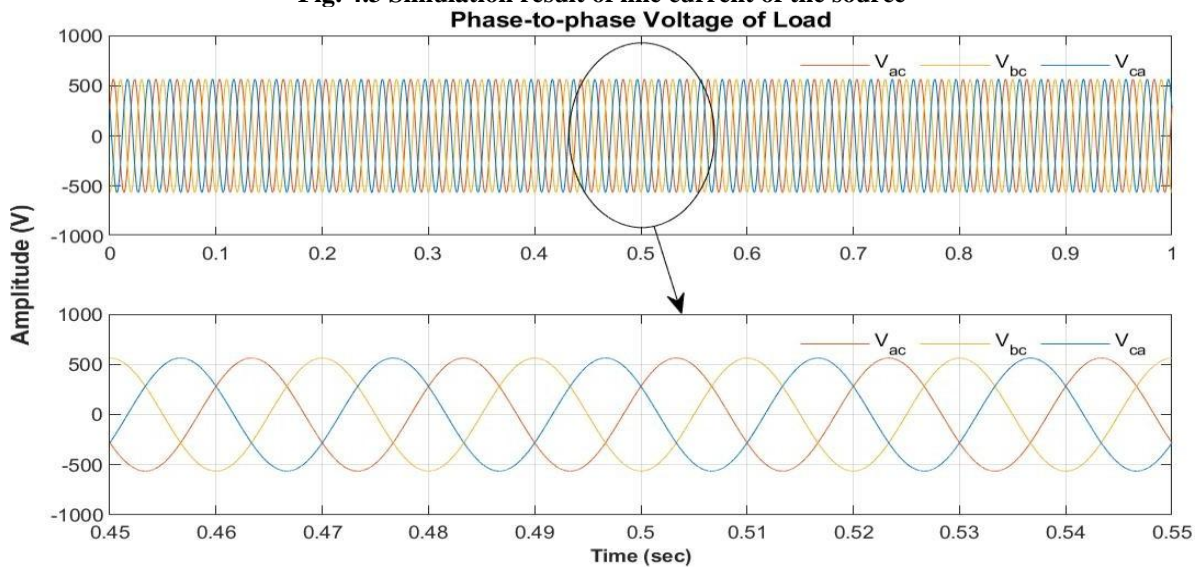


Fig. 4.4 Simulation result of phase-phase voltage of the load

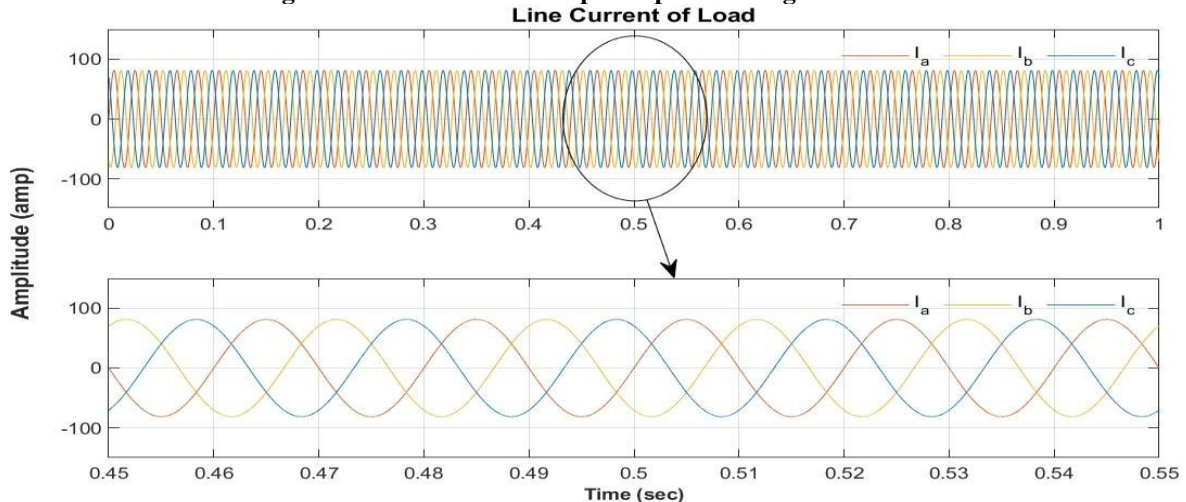


Fig. 4.5 Simulation result of line current of the load

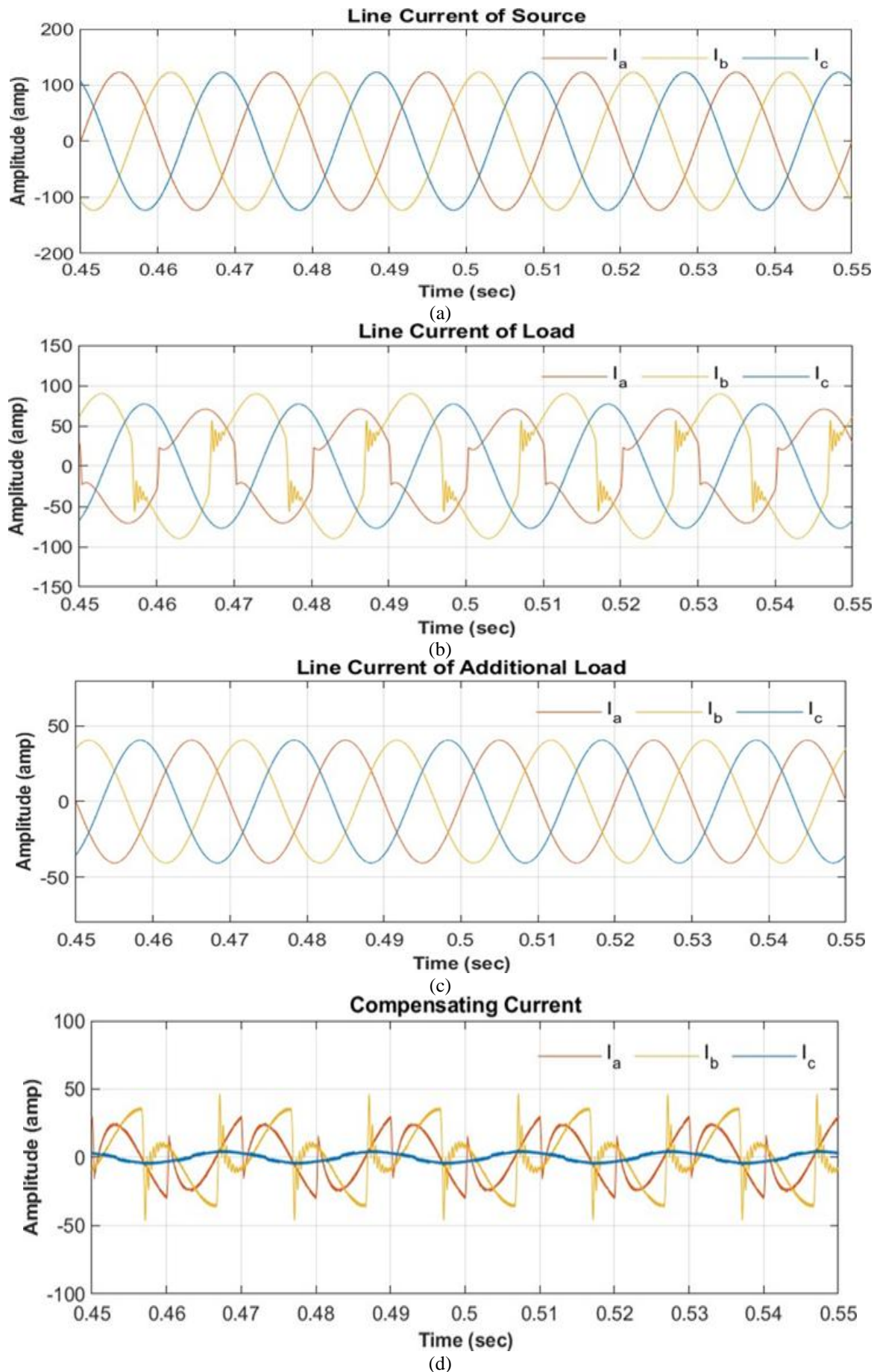


Fig. 4.6 Simulation result of line current of (a) source, (b) load, (c) additional load, respectively and (d) compensating current

Figures 4.6 (a), (b), (c), and (d) show the line currents of the source, load, additional load, and compensating current generated by the ANN-controlled SAPF, respectively, from  $t = 0.45$  sec to  $t = 0.55$  sec. As seen in Fig. 4.6 (d), no harmonics are present, indicating that the SAPF does not need to generate compensating current under linear load conditions.

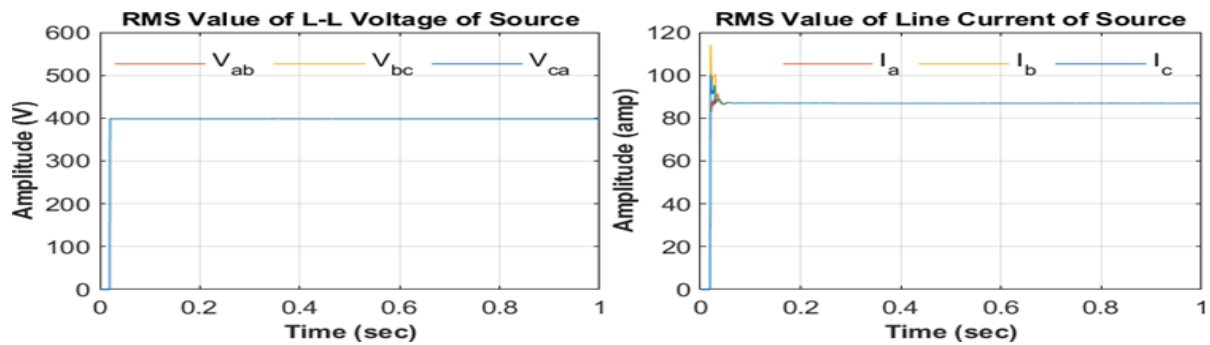


Fig. 4.7 Simulation result of rms value of L-L voltage & current of source, respectively

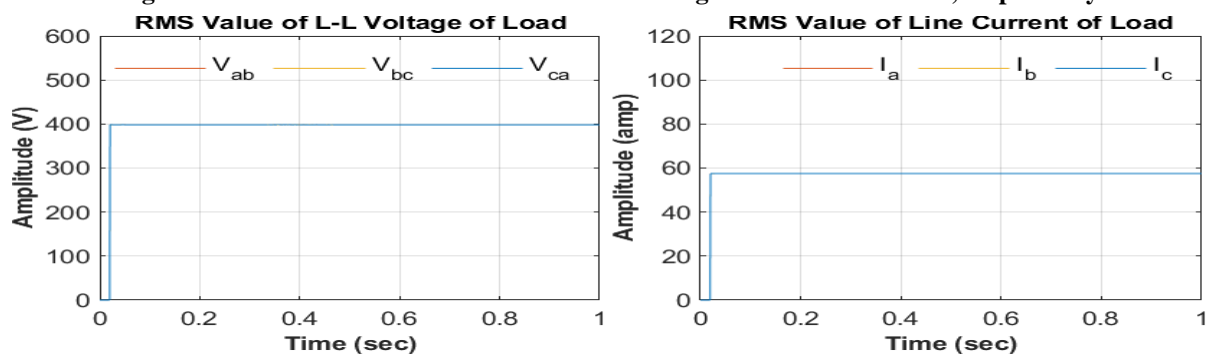


Fig. 4.8 Simulation result of rms value of L-L voltage & current of load, respectively

Figures 4.7 and 4.8 display the RMS values of the line-to-line voltage and current for the source and load, respectively, with constant irradiance throughout the time period. The figures clearly show that no harmonics are present. The RMS voltage for both the load and source is 400 V, with source and load currents around 84 A and 58 A, respectively.

### Case-2: Simulation response of 3- $\Phi$ PI-Controlled SAPF at Non- Linear Load Condition

The simulation results for the PI-controlled SAPF are obtained under nonlinear load conditions. The system consists of two parallel-connected loads: a 40 kW load with unbalanced conditions created using electronic power switches and inductive elements, and a 20 kW balanced (linear) load. This setup is designed to assess the performance of the PI-controlled SAPF and compare it with the proposed control scheme in managing power quality under unbalanced nonlinear load scenarios. The simulation results, shown in the following figures, highlight the performance of the PI-controlled SAPF.

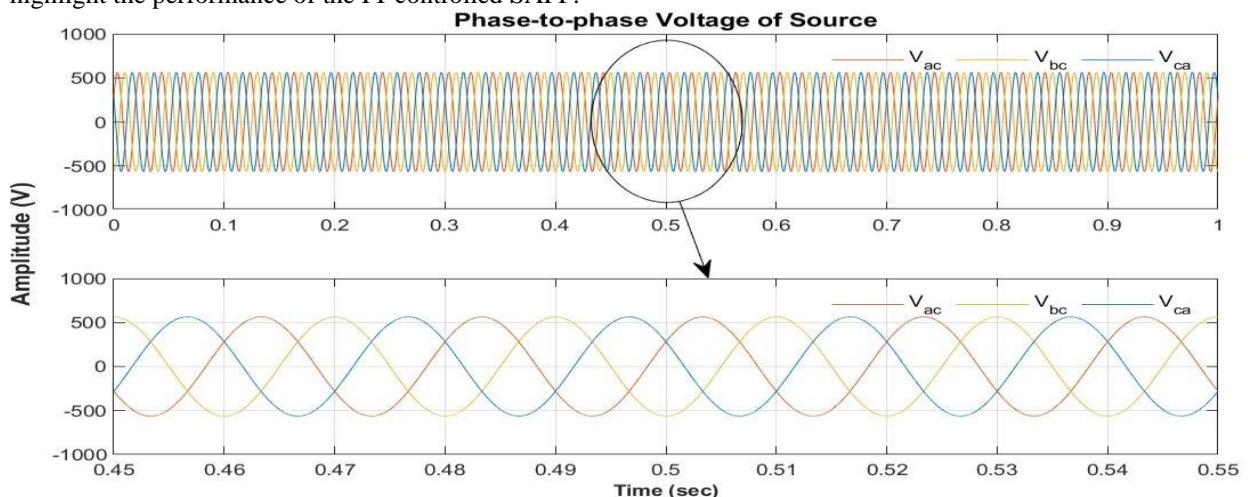
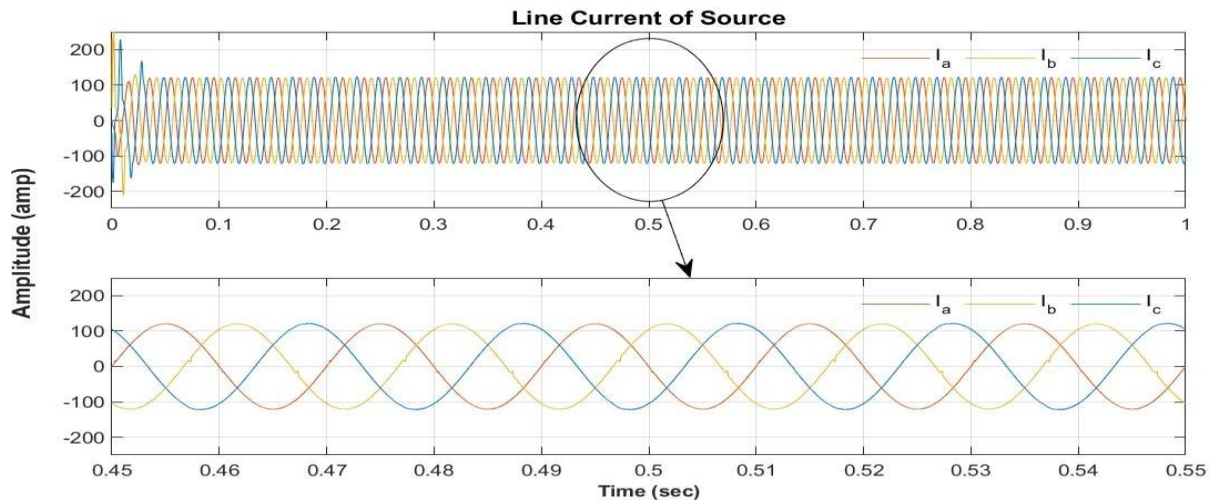


Fig. 4.9 Simulation result of phase-phase voltage of the source





**Fig. 4.10 Simulation result of line current of the source**

Figures 4.0 and 4.10 show the phase-to-phase voltage and line current of the source under unbalanced nonlinear load conditions, respectively. To emphasize the quality of the signals, zoomed-in views are included in both figures. Throughout the simulation, the voltage remains around 565 V, and the current is approximately 120 A. The zoomed-in sections, from  $t = 0.45$  sec to  $t = 0.55$  sec, provide a closer look at the signal details, highlighting the waveform characteristics under these conditions.

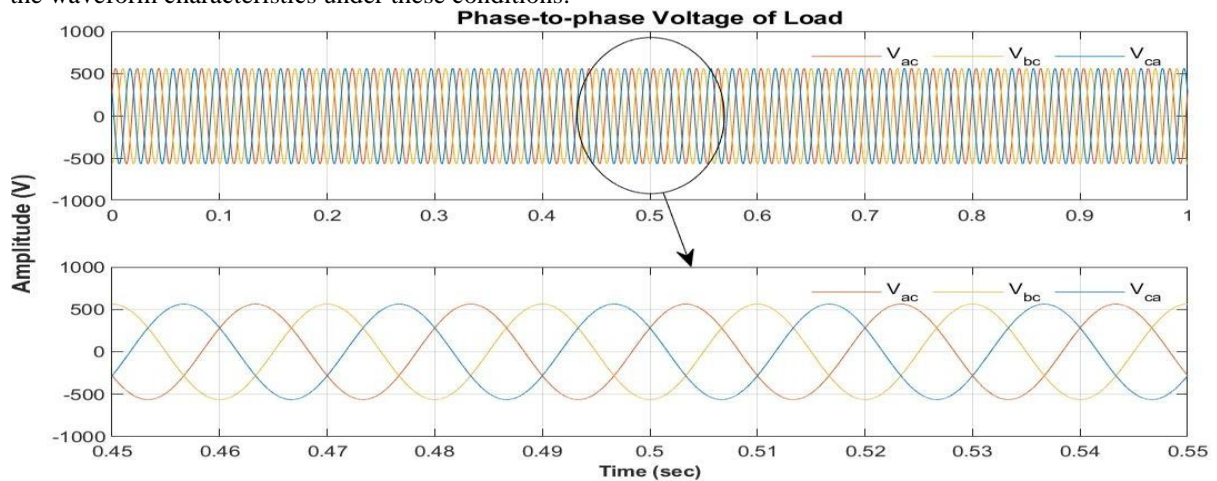


**Fig. 4.11 Simulation result of phase-phase voltage of the load**

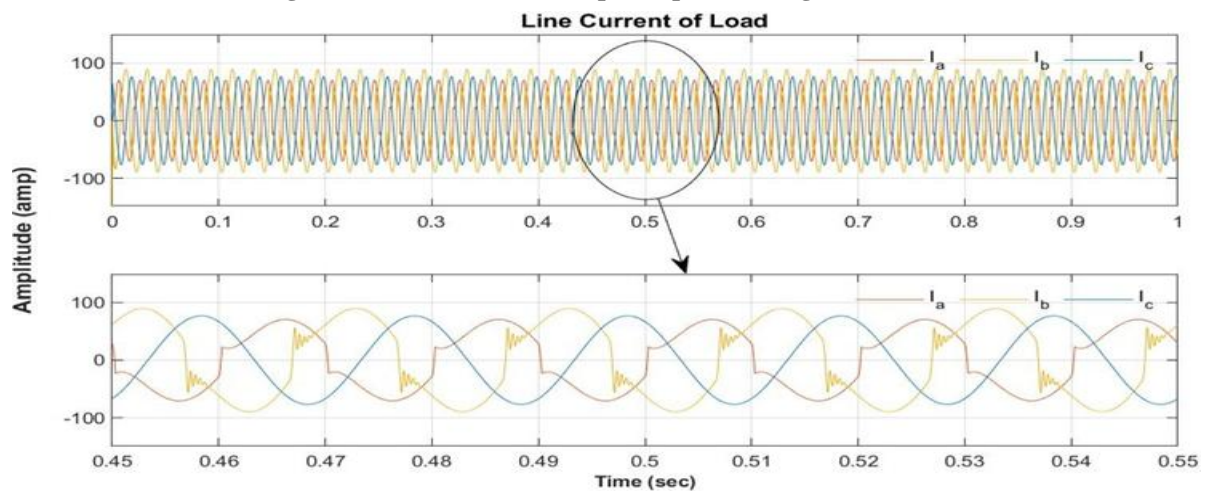


**Fig. 4.12 Simulation result of line current of the load**

Figures 4.11 and 4.12 show the phase-to-phase voltage and line current of the load, respectively. The voltage remains around 565 V, and the current is approximately 80 A throughout the simulation. As seen in Fig. 4.11,

the load current is non-sinusoidal, with harmonics present due to the unbalanced nonlinear load, causing waveform distortions.

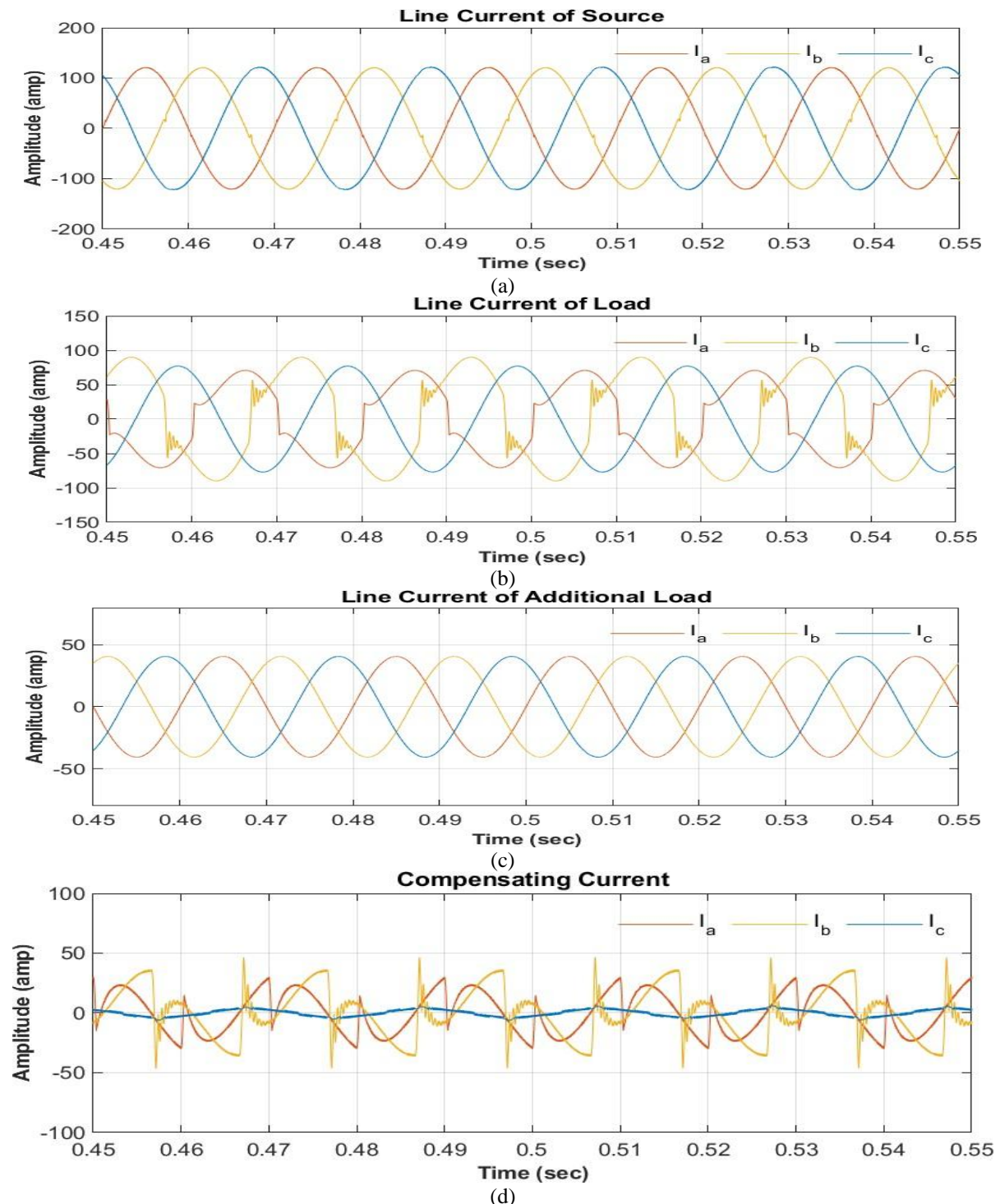


**Fig. 4.13 Simulation result of line current of (a) source, (b) load, (c) additional load, respectively and (d) compensating current**

Figure 4.13 presents the current waveforms for different components of the system under unbalanced nonlinear load conditions, during the time interval from  $t = 0.45$  sec to  $t = 0.55$  sec. The plots include (a) the line current of the source, (b) the line current of the load, (c) the line current of the additional load, and (d) the compensating current generated by the PI-controlled SAPF. The results highlight the system's performance in mitigating the effects of unbalanced nonlinear loads. In Fig. 4.13(b), the load current is non-sinusoidal, with significant harmonic distortion caused by the unbalanced nonlinear load. As a result, the system generates compensating current to correct the source current waveform, as shown in Fig. 4.13(a) and Fig. 4.13(d). However, in Fig. 4.13(a), the source current still shows some distortions due to the PI controller's inability to completely



eliminate harmonics. In Fig. 4.13(c), the additional load remains unaffected by the distortions, demonstrating the SAPF's effectiveness in stabilizing the current waveform. Additionally, the compensating current waveform generated by the proposed instantaneous imaginary power (pq) theory is shown alongside the reference current for the hysteresis controller, indicating that the generated compensating current matches the reference current.

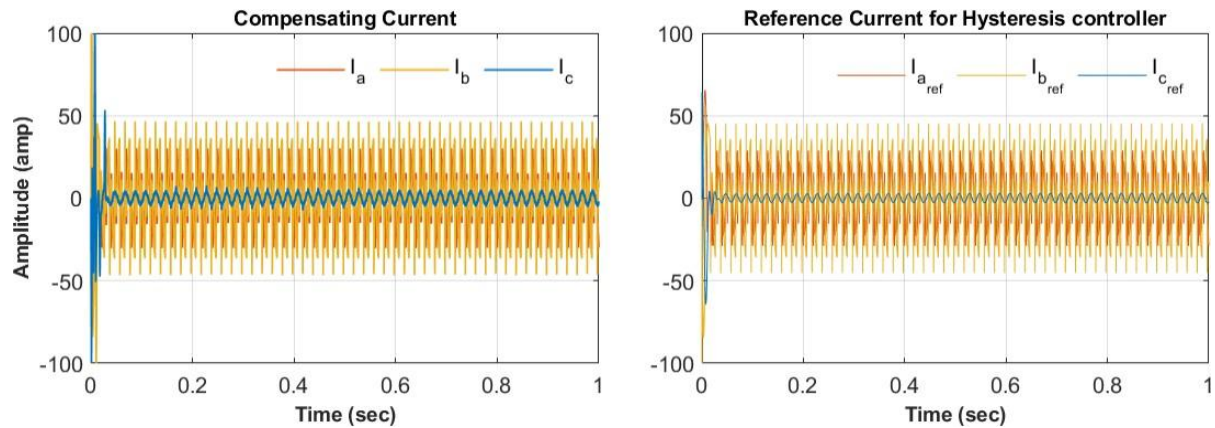


**Fig. 4.14 Simulation results of compensating current and reference current of hysteresis controller**

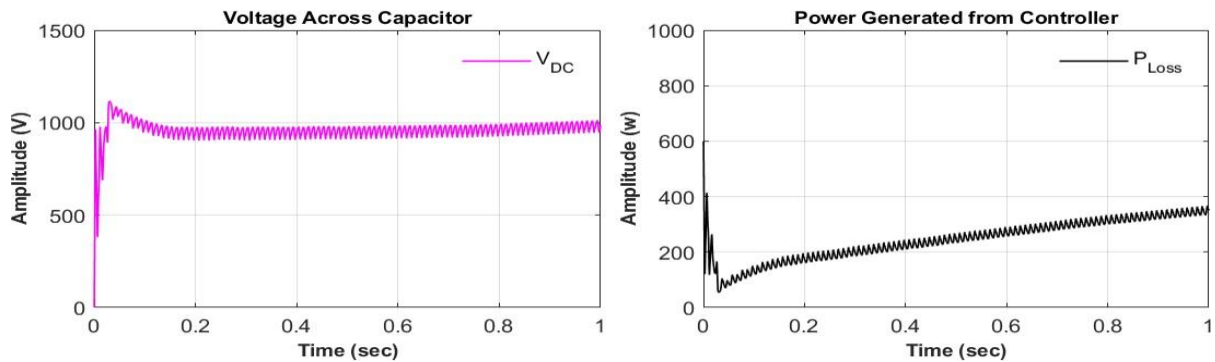


**Fig. 4.15 Simulation results of dc voltage across capacitor and power generated from PI controller**

Fig. 4.15 present the waveform of dc voltage across capacitor and PLoss power generated by the PI controller. The PI controller is maintaining the dc voltage.

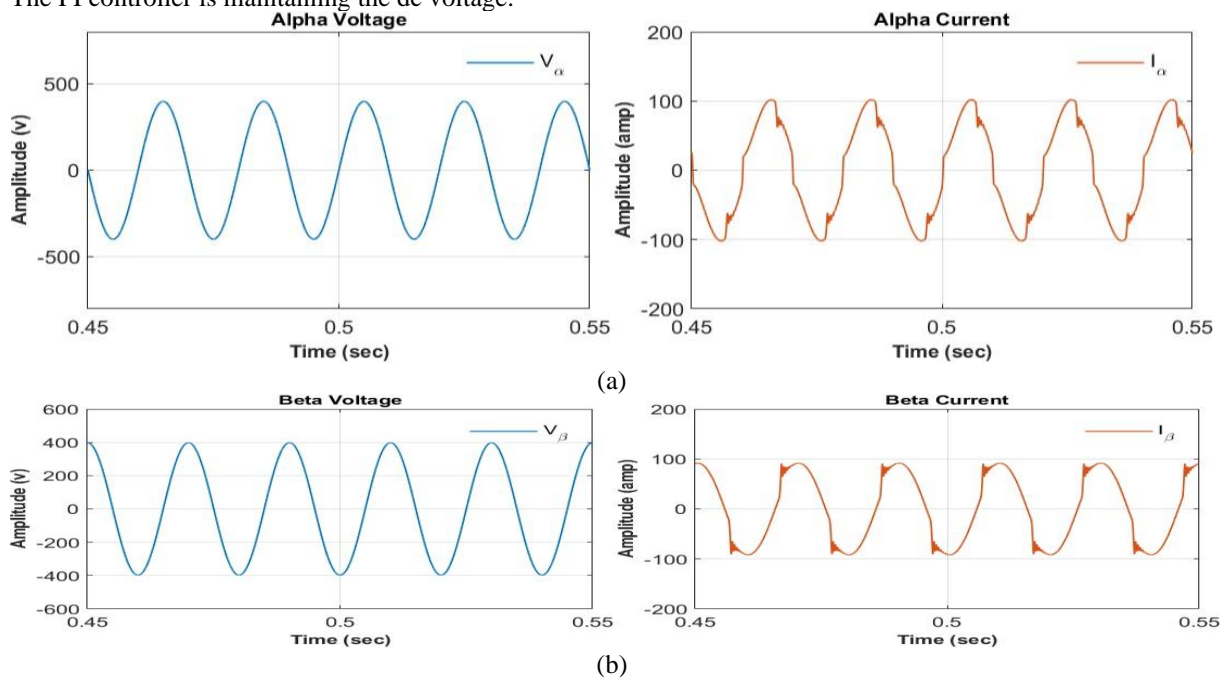


**Fig. 4.16 Simulation results of (a)  $\alpha$  components of voltage & current, (b)  $\beta$  components of voltage and current**

Fig. 4.16 (a) & (b) presents the waveform of  $\alpha$  &  $\beta$  components of the voltage and current, respectively. This  $\alpha$  &  $\beta$  reference current is generated by the clark- transformation block.

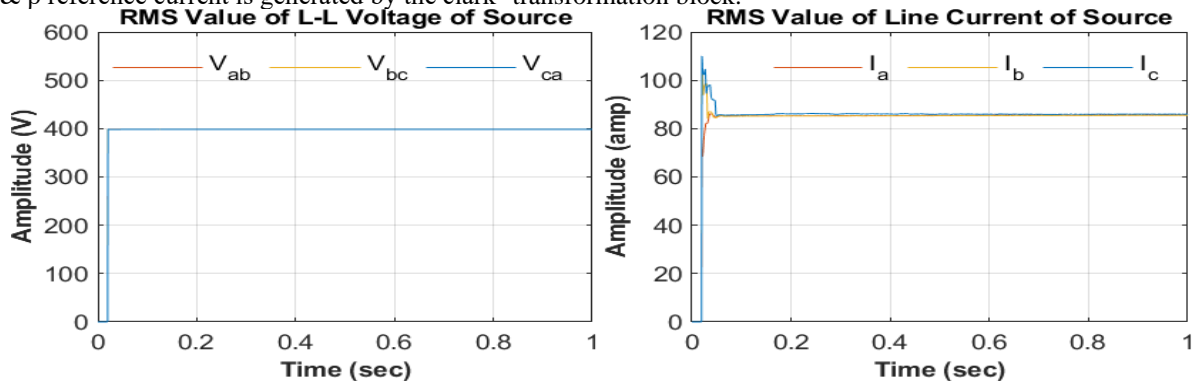


Fig. 4.17 Simulation result of rms value of L-L voltage & current of source, respectively

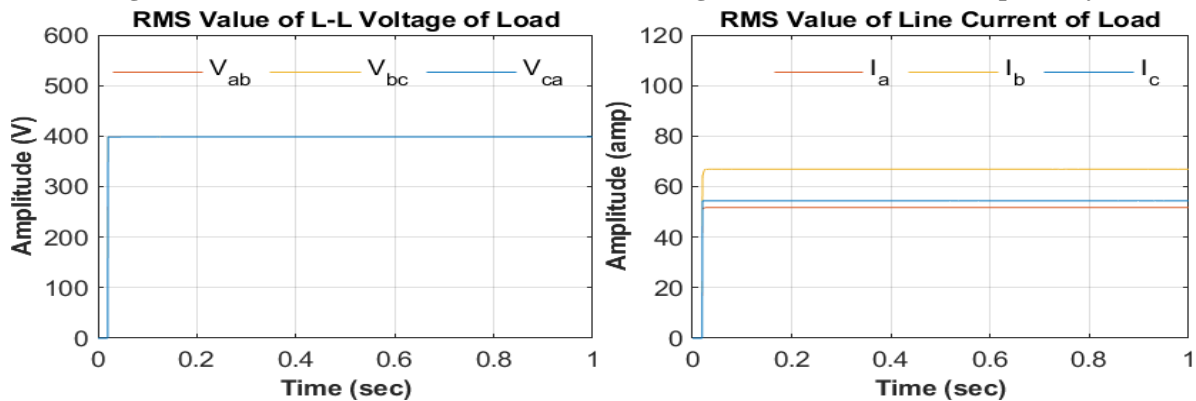


Fig. 4.18 Simulation result of rms value of L-L voltage & current of load, respectively

Figures 4.17 and 4.18 show the RMS values of the line-to-line voltage and current for the source and load, respectively. The RMS voltage for both the load and source remains constant at approximately 400 V throughout the simulation. However, one phase of the load current shows an imbalance, with harmonics present due to the unbalanced nonlinear load. Additionally, the RMS value of the source current exhibits disturbances, as shown in Fig. 4.17.

#### Case-4: Comparative Study between PI-Controller and ANN- Controller SAPF

The Total Harmonic Distortion (THD) plots are analyzed under nonlinear load conditions to evaluate the performance of different control strategies: without compensation, with PI-controlled SAPF, and with ANN-controlled SAPF. The plot for the uncompensated system shows significant harmonic distortion in the source current due to the nonlinear load. The PI-controlled SAPF reduces THD, but some distortion remains due to its limited ability to manage dynamic and nonlinear conditions. In contrast, the ANN-controlled SAPF significantly lowers THD, demonstrating superior harmonic compensation. This highlights the ANN-based approach's effectiveness in improving power quality and system performance.

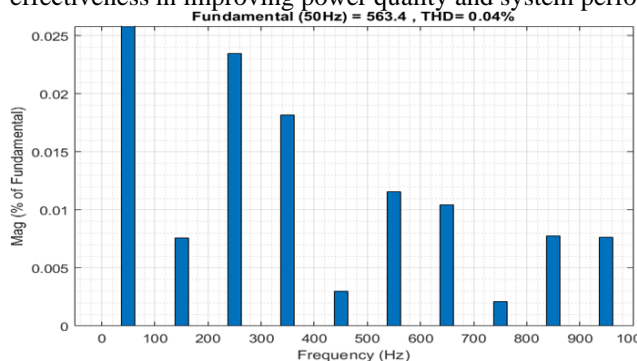


Fig. 4.19 THD plot of source voltage under without compensation

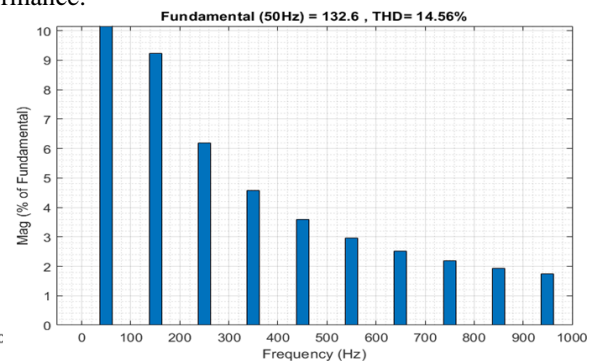
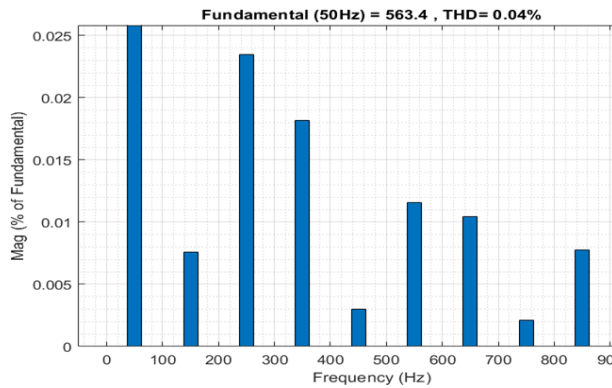


Fig. 4.20 THD plot of source current under without compensation

Figures 4.19 and 4.20 present the Total Harmonic Distortion (THD) plots for the source voltage and source current, respectively, under nonlinear load conditions without compensation. In Fig. 4.19, the THD for the source voltage is minimal, at only 0.04%, with a fundamental value of 563.4 V, indicating negligible voltage

distortion and a nearly pure source voltage waveform despite the nonlinear load. However, Fig. 4.20 shows a significantly higher THD of 14.56% for the source current, with a fundamental value of 132.6 A, highlighting the considerable harmonic distortion caused by the nonlinear load, which negatively impacts power quality. Figures 4.21 and 4.22 show the THD plots for the nonlinear load voltage and current. The load voltage in Fig. 4.21 has minimal distortion, with a THD of 0.04% and a fundamental value of 563.4 V. In contrast, Fig. 4.22 shows a high THD of 20.89% for the load current, with a fundamental value of 92.59 A, reflecting the significant harmonic distortion from the nonlinear load.



**Fig. 4.21 THD plot of load voltage under without compensation**

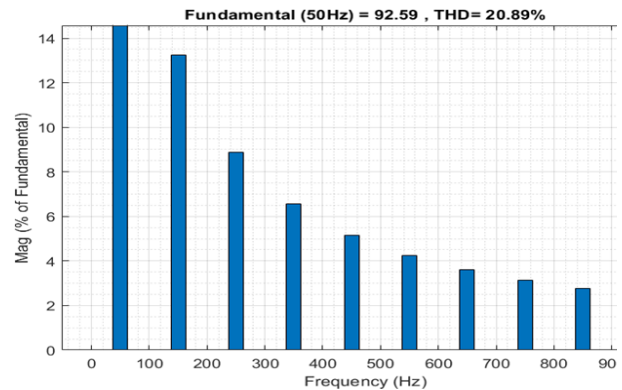


**Fig. 4.22 THD plot of load current under without compensation**

These results underscore the substantial effect of the nonlinear load on the current waveform, highlighting the importance of compensation mechanisms such as the ANN-controlled SAPF to mitigate harmonic distortion and enhance the overall power quality of the system.

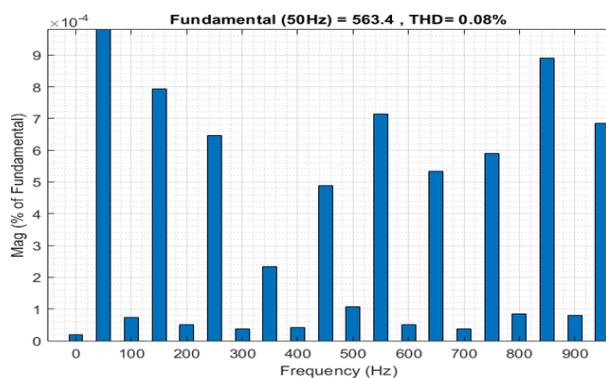


**Fig. 4.23 THD plot of source voltage under PI-controller compensation**

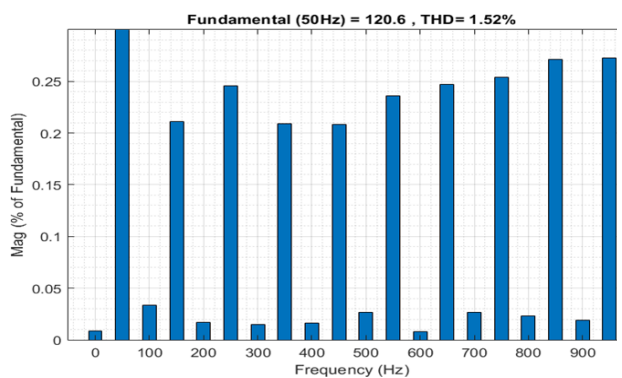


**Fig. 4.24 THD plot of source current under PI-controller compensation**

Figures 4.23 and 4.24 present the Total Harmonic Distortion (THD) plots for the source voltage and source current, respectively, under nonlinear load conditions with PI-controller compensation. In Fig. 4.23, the THD for the source voltage is 0.08%, with a fundamental value of 563.4 V, indicating that the voltage waveform remains nearly pure, showcasing the PI controller's effectiveness in maintaining voltage quality. Fig. 4.24 shows the THD for the source current, reduced to 1.52% with a fundamental value of 120.6 A. While this represents an improvement over the uncompensated scenario, residual harmonic distortion persists, revealing the PI controller's limitations in fully addressing nonlinear load effects.

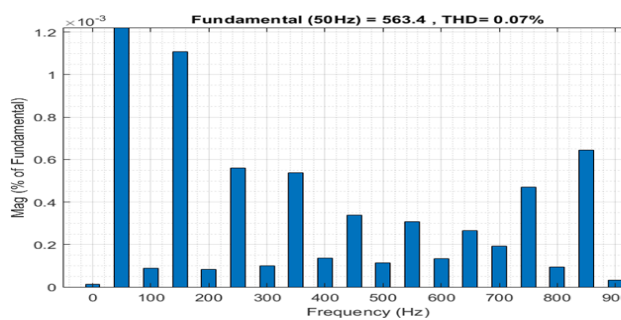


**Fig. 4.25 THD plot of load voltage under PI-controller compensation**

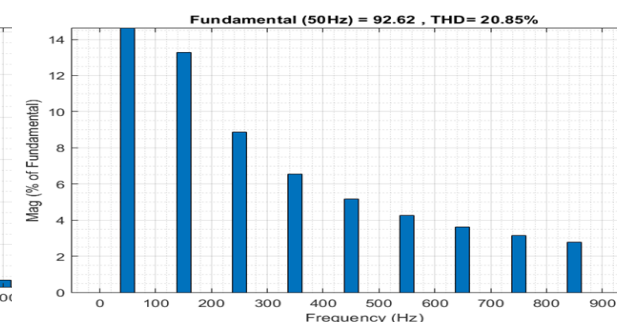


**Fig. 4.26 THD plot of load current under PI-controller compensation**



Figures 4.25 and 4.26 show the THD plots for the load voltage and load current, respectively. In Fig. 4.25, the THD for the load voltage remains low at 0.07%, with a fundamental value of 563.4 V, indicating minimal distortion. However, Fig. 4.26 shows a high THD of 20.85% for the load current, reflecting the inherent harmonic distortion of the nonlinear load. These results demonstrate the PI controller's ability to improve source current quality while maintaining voltage quality. However, its limitations in fully mitigating harmonics highlight the need for advanced compensation mechanisms like the ANN-controlled SAPF for better performance. Figures 4.27 and 4.28 present the THD plots for the source voltage and current under nonlinear load conditions with ANN-controlled SAPF compensation.

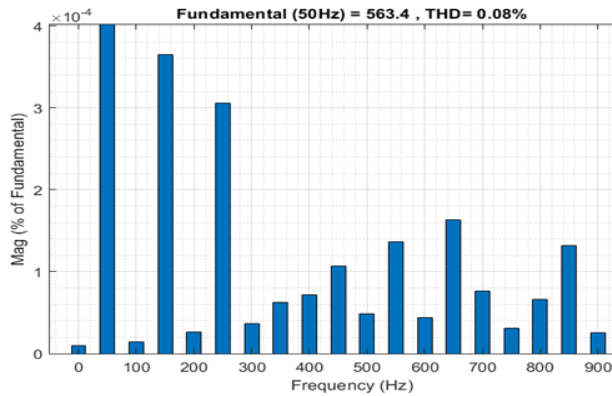


**Fig. 4.27 THD plot of source voltage under ANN-controller compensation**

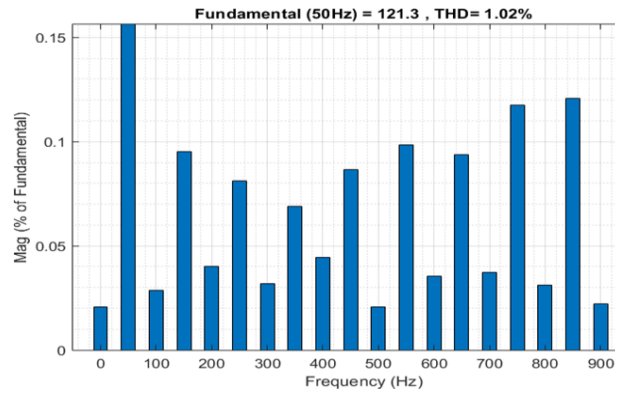


**Fig. 4.28 THD plot of source current under ANN-controller compensation**

In Fig. 4.27, the THD for the source voltage is reduced to an impressive 0.04%, with a fundamental value of 563.4 V, showcasing the ANN controller's ability to maintain a nearly pure voltage waveform and ensuring excellent voltage quality under nonlinear load conditions. Fig. 4.28 demonstrates a significant reduction in the THD for the source current to 1.02%, with a fundamental value of 121.3 A, highlighting the ANN controller's effectiveness in mitigating harmonic distortion and achieving a nearly sinusoidal current waveform.

Figures 4.29 and 4.30 present the THD for the load voltage and current. The load voltage THD is minimal at 0.04%, but the load current exhibits a high THD of 20.85%, which is intrinsic to the nonlinear load and unaffected by the compensation mechanism.

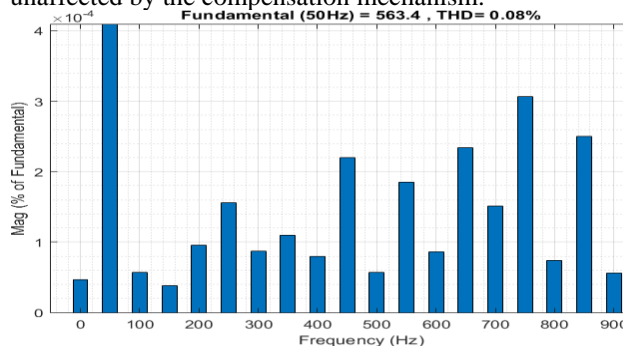


**Fig. 4.29 THD plot of load voltage under ANN-controller compensation**

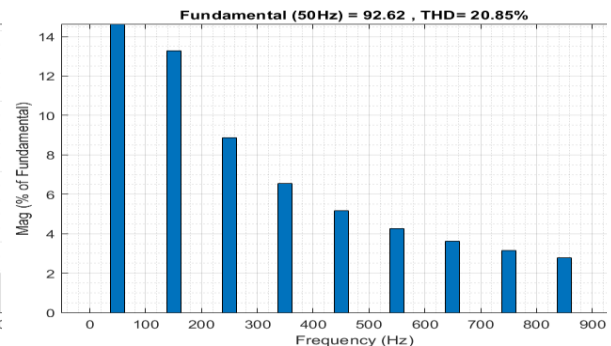


**Fig. 4.30 THD plot of load current under ANN-controller compensation**

These results clearly highlight the superior performance of the ANN-controlled SAPF over traditional PI controllers. The ANN controller not only significantly enhances source current quality but also maintains exceptional voltage quality, effectively mitigating harmonics caused by nonlinear loads. Its advanced compensation mechanism positions it as a highly effective solution for managing power quality in modern power systems.

**Table-4.1 Comparison data between without compensation, with PI-controlled compensation and ANN-controlled compensation under non-linear load condition**

S. No.	Parameters	Non-linear Load		
		Without Compensation	With PI- Controlled Compensation	With ANN- Controlled Compensation
1.	Source Voltage (VS)	0.04%	0.08%	0.08%

2.	Source Current (IS)	14.56 %	1.52%	1.02%
3.	Load Voltage (VL)	0.04%	0.07%	0.08%
4.	Load Current (IL)	20.89 %	20.85%	20.85%

Table 4.1 presents a comparative analysis of the PI-controlled SAPF, ANN-controlled SAPF, and the no-compensation scenario under nonlinear load conditions. The analysis reveals that while the PI-controlled SAPF improves source current THD and maintains source voltage quality, the ANN-controlled SAPF outperforms it by achieving significantly lower THD values for both source voltage and current, ensuring near-perfect sinusoidal waveforms. The "without compensation" scenario shows high THD and degradation in voltage quality, emphasizing the need for effective compensation. These results validate the ANN-controlled SAPF's superior performance in enhancing power quality, making it a robust solution for modern power systems.

## CONCLUSION

- ✓ The source current exhibits significant harmonic distortion (THD of 14.56%) due to nonlinear loads, leading to degraded power quality.
- ✓ Minimal distortion is observed in the source voltage (THD of 0.04%), indicating the adverse effects are primarily on the current waveform.
- ✓ The PI-controller significantly reduces the source current's THD to 1.52%, improving power quality.
- ✓ However, residual harmonics persist, reflecting the PI controller's limited capability to handle dynamic and nonlinear conditions effectively.
- ✓ The ANN-controlled SAPF reduces the source current's THD to 1.02%, achieving a near-sinusoidal waveform and outperforming the PI controller.
- ✓ It maintains excellent source voltage quality (THD of 0.04%), demonstrating its superior adaptability to nonlinear load conditions.
- ✓ Both controllers maintain minimal THD for the load voltage, indicating no significant voltage distortion due to compensation mechanisms.
- ✓ The load current retains high THD values (~20.85%) across all scenarios, as this distortion is intrinsic to the nonlinear load and independent of compensation.
- ✓ The ANN-controlled SAPF excels in reducing source current distortion and maintaining superior voltage quality compared to the PI-controlled SAPF.
- ✓ The advanced dynamic and adaptive capabilities of ANN make it a robust solution for addressing harmonic distortions in modern power systems.

## REFERENCES

- [1] Govind A; Jayaswal K; Tayal V.K and Kumar P. "Simulation and real time implementation of shunt active power filter for power quality enhancement using adaptive neural network topology" *Electric Power Systems Research*, vol. 228, no. 1, pp. 1-14, 2024.
- [2] Rao, P; Prakash K and Suryakalavathi M. "A Dynamic Power Quality Enhancement Modeling of Hybrid Active Power Filter Using Artificial Intelligence Controller" *Industrial Engineering Journal*, vol. 53, no. 6, pp. 61-69, 2024.
- [3] Imam A.A; Kumar S.R and Al-Turki Y.A. "Modeling and Simulation of a PI Controlled Shunt Active Power Filter for Power Quality Enhancement Based on P-Q Theory" *Electronics*, vol. 9, no. 4, pp. 1-17, 2020.
- [4] Mahaboob, S.; Ajithan, S.; Jayaraman, S. "Optimal design of shunt active power filter for power quality enhancement using predator-prey based firefly optimization. *Swarm*" *Evol. Comput.* vol. 44, no. 1, 2018. [CrossRef]
- [5] Sundaram, E.; Venugopal, M. "On design and implementation of three phase three level shunt active power filter for harmonic reduction using synchronous reference frame theory". *Int. J. Electr. Power Energy Syst.* vol. 81, pp. 40-47, 2016. [CrossRef]
- [6] Chaoui, A.; Gaubert, J.-P.; Krim, F. Power quality improvement using DPC controlled three-phase shunt active filter. *Electr. Power Syst. Res.* vol. 80, pp. 657-666, 2010. [CrossRef]
- [7] Singh, B., Al-Haddad, K., & Chandra, A. "A review of active filters for power quality improvement", *IEEE Transactions on Industrial Electronics*, vol. 46, no. 5, pp. 960-971, Oct. 1999.
- [8] Sravanthi, K. and Sujatha, C. "A Novel Shunt Active Filter Algorithms for a Three Phase System with Unbalanced Distorted-Source Voltage Waveforms Feeding an Adjustable Speed Drive", *International Journal of Power Control Signal and Computation*, vol. 2, no. 2, pp.112-118, 2015.
- [9] Charles, S. and Bhuvaneshwari, G. "Comparison of three phase shunt active power filter algorithms",

- International Journal of Computer and Electrical Engineering, vol. 2, no. 1, pp. 175- 180, Feb. 2010.
- [10] Litran, S. P., Salmeron, P., Vazquez, J. R. and Flores, J. L. "Compensation of voltage unbalance and current harmonics with a series active power filter", *Renewable Energy & Power Quality Journal*, vol.1, no. 3, pp. 222-227, Mar. 2005.
- [11] Litran, S. P., Salmeron, P., Vazquez, J. R. and Herrera, R. S. "Different control strategies applied to series active filters", *IEEE International Symposium*, Jul. 2007.
- [12] Chen, L. and Jouanne, A. V. "A comparison and assessment of hybrid filter topologies and control algorithms", *IEEE Annual Power Electronics Specialists Conference*, held at Vancouver, BC, Canada during June 17-21, pp. 565-570, 2001.
- [13] Karthik, K. and Quaicoe, J.E. "Voltage compensation and harmonic suppression using series active and shunt passive filters", *IEEE Canadian Conference on Electrical and Computer Engineering*, held at Halifax, NS, Canada, Canada during May 7-10, pp. 582-586, 2000.
- [14] Kumar, S., Solanki, S., Kumar, P. (2025). Voting Regression Model for the Air Quality Prediction. In: Singh, R., Gehlot, A. (eds) *Business Data Analytics. ICBDA 2023. Communications in Computer and Information Science*, vol 2358. Springer, Cham.  
[https://doi.org/10.1007/978-3-031-80778-7\\_5](https://doi.org/10.1007/978-3-031-80778-7_5)
- [15] Singh, G., Kalra, M., Kumar, R., Kumar, P. (2025). Diabetic Retinopathy Detection Approach Using Convolution Neural Networks. In: Singh, R., Gehlot, A. (eds) *Business Data Analytics. ICBDA 2023. Communications in Computer and Information Science*, vol 2358. Springer, Cham.  
[https://doi.org/10.1007/978-3-031-80778-7\\_4](https://doi.org/10.1007/978-3-031-80778-7_4)
- [16] Upadhyay, K.G., Kalra, M., Kumar, R., Kumar, P. (2025). A Novel Approach for Diabetic Prediction Using Attribute Subset Selection, K-Means and Logistic Regression. In: Singh, R., Gehlot, A. (eds) *Business Data Analytics. ICBDA 2023. Communications in Computer and Information Science*, vol 2358. Springer, Cham.  
[https://doi.org/10.1007/978-3-031-80778-7\\_3](https://doi.org/10.1007/978-3-031-80778-7_3)
- [17] L. Jhala et al., "Development of Control Strategy for Power Management in Hybrid Renewable Energy System" *International Journal of Technical Research and Science*, vol. VI, Issue XII, Dec. 2021.
- [18] Singh, M. and Tiwari, V. "Modeling analysis and solution of power quality problems", *National Level Conference Problem Practices and Prospects in Power Distribution System Operation and Control*, vol. 5, pp.121-132, 2012.
- [19] Karuppanan, P. & Mahapatra, K. "PLL with PI, PID and Fuzzy Logic Controllers based Shunt Active Power Line Conditioners", *IEEE International Conference on Power Electronics, Drives and Energy Systems*, held at New Delhi, India during Dec. 20-23, pp-1-6, 2010.
- [20] S. Sharma; R. Jangid and K. Parikh "Development of Intelligent Control Strategy for Power Quality Improvement of Hybrid RES Using AI Technique" *International Journal of Technical Research and Science*, vol. VIII, Issue II, Feb. 2023.
- [21] Tamilvani, M., Nithya, K. and Srinivasan, M. "Harmonic Reduction in Variable Frequency Drives Using Active Power Filter", *Telkomnika Indonesian Journal of Electrical Engineering*, vol. 12, no. 8, pp. 5758-5765, Aug. 2014.
- [22] Tang, Y., Loh, P. C., Wang, P., Choo, F. H., Gao, F., & Blaabjerg, F. "Generalized Design of High Performance Shunt Active Power Filter With Output LCL Filter", *IEEE Transactions on Industrial Electronics*, vol. 59, no. 3, pp. 1443-1452, March-2012.
- [23] Bhattacharyya, S., Cobben, S., Ribeiro, P. and Kling, W. "Harmonic emission limits and responsibilities at a point of connection", *IET Generation, Transmission & Distribution*, vol. 6, no. 3, pp. 256–264, March-2012.
- [24] Choe, J. H and Park, M. H. "A new injection method for AC harmonic elimination by active power filter", *IEEE Transactions on Industrial Electronics*, vol. 35, no.1, pp. 141–147, Feb. 1988.
- [25] S. Kumar: R. Jangid and K. Parikh "Comparative Performance Analysis of Adaptive Neuro-Fuzzy Inference System (ANFIS) & ANN Algorithms Based MPPT Energy Harvesting in Solar PV System." *International Journal of Technical Research and Science*, vol. 8, Issue 3, March 2023.
- [26] Shankar, M., Monisha, S., Shesna, H., Vignesh, T., Sikkandar, N., Sundaramoorthi, S. and Venkatesh, S. "Implementation of Space Vector Pulse Width Modulation Technique with Genetic Algorithm to Optimize Unified Power Quality Conditioner", *American Journal of Applied Sciences*, vol. 11, no. 1, pp. 152-159, 2014.
- [27] Ghani, M. A. "A simple active power filter with 5-level NPC inverter", *International Conference on Engineering Technology and Technopreneurship*, Kuala Lumpur, pp. 330-334, 2014.
- [28] R. Jangid; J.k Maherchandani; V.K Yadav and R.K Swami, "Energy Management of Standalone Hybrid Wind-PV System", *Journal of Intelligent Renewable Energy Systems (John Wiley & Sons, Inc.)* Pages 179- 198, 2022.